Journal of Sustainability Science and Management
Volume 20 Number 10, October 2025: 2021-2038
eISSN: 2672-7226

THE IMPACT OF THERMAL STRATIFICATION ON NUTRIENT AND GREENHOUSE GAS DISTRIBUTION IN A DEEP TROPICAL RESERVOIR

SITI FARHAIN MOHD LUDIN[1], DARYL LEE JIA JUN[1], WEI WEN WONG[3] AND SENG CHEE POH[1,2]*

[1]*Faculty of Science and Marine Environment, Universiti Malaysia Terengganu, 21030 Kuala Nerus, Terengganu, Malaysia.*
[2]*Institute of Oceanography and Environment, Universiti Malaysia Terengganu, 21030 Kuala Nerus, Terengganu, Malaysia.*
[3]*Water Studies, School of Chemistry, Monash University, 3800 Clayton, Victoria, Australia.*

**Corresponding author: poh@umt.edu.my*
http://doi.org/10.46754/jssm.2025.10.002
Submitted: 6 January 2025 Revised: 25 March 2025 Accepted: 14 April 2025 Published: 15 October 2025

Abstract: This study examines thermal stratification in Kenyir reservoir using data from five sampling campaigns between February and November 2018. Field and lab analysis were carried out to examine water temperature profiles, thermocline parameters, lake number, Schmidt stability, dissolved oxygen, nutrients, and greenhouse gases. Results reveal that stratification persisted throughout the study period, with signs of epilimnetic mixing observed in February and November 2018. CO_2 and CH_4 median concentrations during the dry period were 362 µM and 1.8 µM, higher than in the wet period (175 µM and 1.2 µM). Greenhouse gas concentrations were highest at the bottom layer, with CO_2 and CH_4 levels of 573 µM and 379 µM, respectively, compared to the thermocline (373 µM and 2.6 µM) and surface (179 µM and 0.8 µM). The dissolved inorganic nitrogen and phosphorus concentrations averaged 184 ± 247 µg/L and 7 ± 4 µg/L, respectively, lower than the global average. This study highlights the influence of stratification on greenhouse gas dynamics and nutrient distributions, offering insights for local energy authorities to mitigate climate change impacts. Understanding factors that destabilise stratification can help manage the reservoir's carbon footprint and optimise hydropower sustainability.

Keywords: Malaysia dam, hydropower, carbon dioxide, methane.

Introduction

Over the past few decades, Malaysia has constructed numerous large dams to meet national energy demands. Most of these deep reservoirs experience thermal stratification, resulting in three distinct water layers: The epilimnion, metalimnion (or thermocline), and hypolimnion (Sharip, 2017). Hydropower reservoirs are required to maintain high water levels to ensure sufficient water head for generating hydropower. Compared to other types of reservoirs such as irrigation reservoirs, hydropower reservoirs typically have much longer water residence times. As a result, water density varies with temperature at different depths, leading to the formation of distinct layers that do not mix. Studies indicate that thermal stratification can impact water quality (Noori *et al*., 2018), biochemical cycles of important elements (Beaulieu *et al*., 2014), greenhouse gas emissions (Pu *et al*., 2020), and phytoplankton and microbial community dynamics (Yue *et al*., 2023; Wang *et al*., 2024). Changes in water column physical parameters such as changes in water level can trigger GHG emissions from the water column to the atmosphere (DelSontro *et al*., 2016). These reservoirs can be broadly classified into littoral and limnetic zones based on depth (USEPA, 2002), with stratification patterns influencing physical and biochemical processes across these zones.

Thermal stratification influences the bioavailability and dispersion of dissolved nutrients in several ways. In a stratified system, primary producers assimilate nitrate and convert it into organic biomass in the epilimnion. This biomass eventually settles as particulate organic matter and is aggregated at the metalimnion, some of it is later released back into the water as ammonium (Yang *et al*., 2021). In hypolimnion, hypoxic conditions promote the release of phosphorus and nitrate from lake sediments substantially elevated by increased lake primary productivity and dissolved nutrient supply (Ma *et al*., 2021; Wang *et al*., 2024).

In the hypolimnion, low levels of dissolved oxygen are associated with the decay of organic matter, which potentially fuels the production of methane and carbon dioxide (Zhou *et al*., 2019; Pu *et al*., 2020). Therefore, understanding thermal stratification is essential for dam operators to manage water quality and control greenhouse gas emissions from reservoirs. The Kenyir reservoir supplies water to the Sultan Mahmud hydro power station and is the largest artificial dam in Peninsular Malaysia. At an elevation of 138 m above mean sea level, it spans a surface area of 370 km^2 and has a catchment area of 2,600 km^2. Malaysia experiences the northeast monsoon, the southwest monsoon and two shorter monsoon transitions annually.

Many limnology studies have been carried out in the Kenyir Reservoir. These studies included reservoir water physicochemical dynamics (Wahab *et al*., 2022), rare earth elements (Sultan & Shazili, 2009), heavy metals (Sultan & Shazili, 2009), sediment loading (Abdul Razad *et al*., 2020), Carlson's Trophic State Index (Sharip, 2017), periphyton (Rouf *et al*., 2008; Rouf *et al*., 2010), chlorophyll a and zooplankton (Yusoff *et al*., 2002), and fish communities (Ambak & Jalal, 1998). However, most of these studies focus on surface water or shallow depths (< 20 m) while the reservoir's average depth exceeds 35 m. The influence of thermal stratification on water quality, particularly at deeper layers, remains underexplored. Thus, this study aims to analyse the thermal stratification patterns in a warm tropical reservoir and investigate how these patterns affect the vertical distribution of dissolved oxygen, nutrients, and greenhouse gas concentrations in relation to seasonal rainfall variations (wet vs. dry) and lake zones (limnetic vs. littoral).

Materials and Methods

Study Area

The study was conducted in the Kenyir Reservoir, located in Terengganu, Malaysia. The reservoir has a maximum depth of 145 m and an average depth of 35 m (Kamaruddin *et al*., 2011). The sources of the rivers that were present in the Kenyir Reservoir area such as Terengganu River, Cacing River, Pertang River, Tembat River, Petuang River, and Terengganu River originate from the highlands and forested areas of Terengganu and its neighbouring regions (Wahab *et al*., 2023). These rivers primarily trace their headwaters to the hilly and mountainous terrains of the Titiwangsa Range, which serves as a key watershed area in Peninsular Malaysia. These seasonal variations were analysed using monthly rainfall data obtained from the Malaysian Meteorological Department, Ministry of Natural Resources and Environmental Sustainability (Figure S1).

Water Sampling

Water samples were collected from the main reservoir body at seven different sites (S1 to S7) using a boat. Sites S1, S2, and S7 are in shallow waters (referred to as the littoral zone), with maximum depths of less than 45 m. In contrast, sites S3 to S6 are situated in deeper waters, exceeding depths of 70 m, and are designated as the limnetic zone (Figure 1 & Table 1).

Five sampling campaigns were carried out between the wet season (November and February) and the dry season (March, May, and July) in 2018. Water samples were collected at 4-6 different depths at each site using a five-litre Niskin water sampler. The first depth was at 0.5 m of the surface, the second was at the photic maximum depth determined by Secchi disk readings, the third was midway between the second depth and the bottom, and the final depth was where the dissolved oxygen value reached zero (the anoxia zone) or 2 m above bottom, two addition depths were taken at open water (limnetic) sites. At each site, in-situ depth profile measurements of dissolved oxygen, conductivity, pH, and temperature were taken using a multiparameter sensor (YSI Sonde 6600, USA) at a sampling interval of 1 m. The collected water samples were filtered through a 0.2 µm PES membrane filter, kept in 250-mL acid-cleaned HDPE bottles and frozen (-20 °C) until further nutrient analysis in the laboratory.

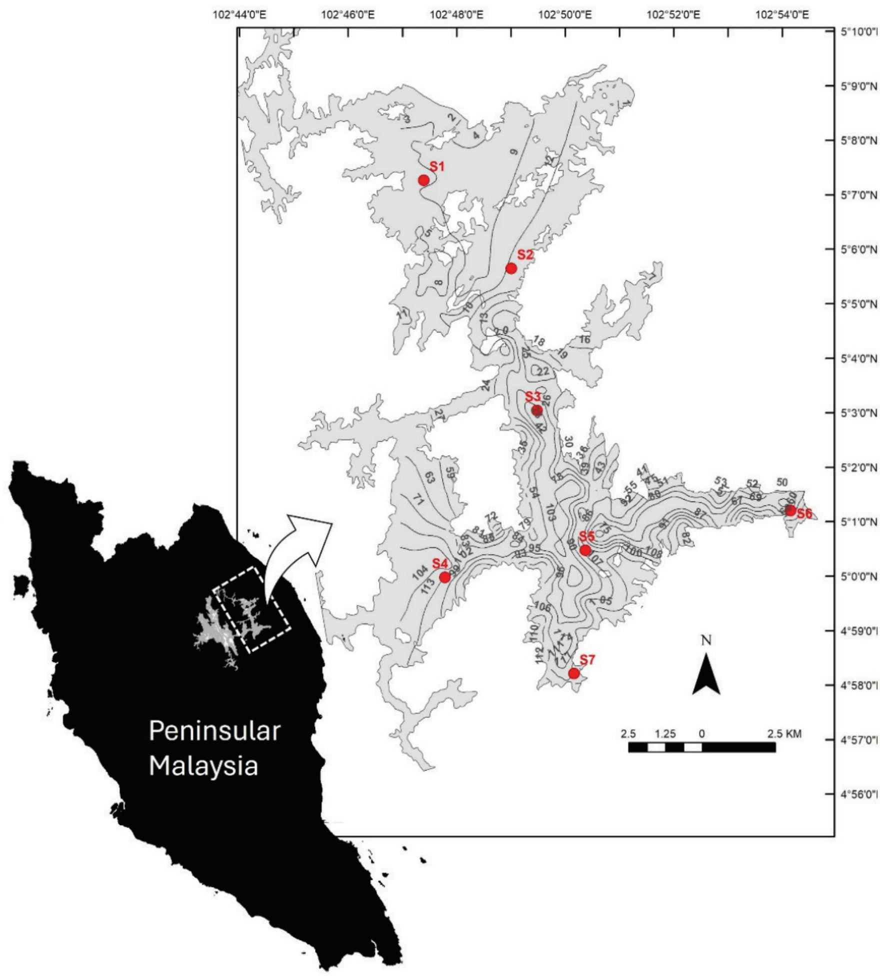

Figure 1: Bathymetry of Kenyir Reservoir (black contours, m) with study sites marked in red

Table 1: The sampling latitude, longitude, and depth in Kenyir Lake

Station	Latitude	Longitude	Maximum Depth (m)	Photic Depth (m)
S1	5.121071	102.7899	35	3.2
S2	5.09414	102.8169	40	3.0
S3	5.050751	102.8248	110	3.1
S4	4.999661	102.7965	130	3.5
S5	5.007959	102.8397	140	3.5
S6	5.020104	102.9027	70	3.4
S7	4.966159	102.8371	45	3.0

Nitrate (NO_2-N) and Nitrite (NO_3-N) Analysis

The measurement of the nitrate and nitrite concentration in water samples was analysed following the Garcia-Robledo *et al*. (2014) method. This analysis involved two steps. First, all the nitrate in the sample was reduced to nitrite by adding vanadium (III) chloride (VCl_3). The reduction of NO_3^- to NO_2^- allowed both NO_3- (after reduction to NO_2^-) and existing NO_2^- to be detected using the Griess reaction technique, as the complete reaction generates a red azo dye with maximum absorption at 504 nm. The absorbance of the sample was measured with a Varian Cary 50 UV-Visible (UV-VIS) Spectrophotometer.

Ammonium (NH_4-N) Analysis

Ammonium concentration was determined by the colourimetric method (USEPA, 1993). This method involves adding an oxidising solution (alkaline citrate + sodium hypochlorite) to convert ammonium ions into samples to free ammonia. Hypochlorous acid (HOCl) and an alkaline phenol solution were added to the sample to convert the free ammonia into indophenol blue monochloramine. The blue colour was intensified with the presence of sodium nitroprusside. The absorbance was measured at 640 nm with a UV-VIS spectrophotometer.

Dissolved Reactive Phosphorus (DRP) Analysis

Phosphorus in water samples was measured by reacting with ammonium molybdate and potassium antimonyl tartrate in an acid medium (5N sulfuric acid) to form phosphomolybdic acid, which was then reduced to molybdenum blue by ascorbic acid (0.01 M). Details of the method can be found in (USEPA, 1993b). The blue solution absorbance was measured at 880 nm using a UV-VIS spectrophotometer.

Dissolved Organic Carbon (DOC) Analysis

One litre of the water sample was filtered through a GF/F Whatman glass microfiber filter paper (0.7 µm). The filtrates were acidified with 37% hydrochloric acid until a pH of two was reached to remove all the dissolved inorganic carbon. The sample was then introduced to the total organic carbon analyser (SHIMADZU TOC-L, Japan) to determine the Dissolved Organic Carbon (DOC) concentration in water samples.

Particulate Organic Carbon (POC) Analysis

For Particulate Organic Carbon (POC) measurement, the suspended solids on the GF/F filters were determined using the loss-on-ignition method (Barillé-Boyer *et al*., 2003). In general, the GF/F filter paper was pre-weighed and kept in a glass desiccator (each filter paper was placed in a labelled stainless steel round plate covered with aluminium foil) to protect samples from humidity. After filtration, the filter papers were oven-dried at 105°C for two hours and cooled to room temperature inside the desiccator.

The filter papers were weighed on an analytical balance to four decimal places. The concentration of Suspended Particulate Matter (SPM) in the sample was calculated by the weight difference of the filter paper before and after filtration divided by the filtrate volume. The SPM can be divided into POC and Particulate Inorganic Carbon (PIC). By combusting the filter samples in a muffle furnace at 450°C for four hours, the organic fraction of SPM was burnt off, and the weight loss of the filters represents the POC. The filter papers were then cooled to room temperature in glass desiccators before weighing for the final weight.

Methane (CH_4) and Carbon Dioxide (CO_2) Analysis

A 60 mL sample of greenhouse gases was carefully filled to the brim of a serum bottle at the site. All samples were collected in triplicate. The samples were preserved with saturated $HgCl_2$ before being crimped with butyl septa and kept at room temperature until further analysis (Lee *et al*., 2022). The greenhouse gas samples were headspace by replacing one-third of the water with helium gas. The samples were then left to equilibrate at room temperature for 30 minutes, followed by CO_2 and CH_4 measurements using a gas chromatograph (Agilent 7980 GC system) equipped with a Flame Ionisation Detector (FID) and Thermal Conductivity Detector (TCD). 5 mL of headspace was injected into the GC using a gas-tight syringe. The GC was equipped with a 0.9 m by 1.6 cm o.d. column packed with 80/100 mesh HayeSep Q (Agilent J&W). For CH_4 analysis, Helium carrier gas was set at a flow rate of 21 mL min^{-1}. The FID operated under the following conditions: N_2 makeup gas two mL min^{-1}, H_2 48 mL min^{-1}, air 500 mL min^{-1}, temperature 250°C. CO_2 concentration was measured by a GC-TCD detector operated at the column temperature of 120°C and detected filament temperature of 200°C. The GC column oven was operated with an initial temperature of 50°C for four minutes and then programmed to 90°C and held at this temperature for six minutes. Quantification was performed by 8-point calibrations from 1 to 2,000 ppm for CH_4 and 1 to 3,000 ppm for CO_2 in nitrogen. High-concentration samples were diluted using high-purity nitrogen.

Schmidt Stability Index (S_t)

The Schmidt stability index (S_t) is a proxy to quantify the energy required to fully mix a thermally stratified lake (expressed in the unit of J/m^2), equation 1.

$$S_t = \frac{g}{A_0}\sum_{z_0}^{z_m}\left(z - z_{\bar{p}}\right)\left(p_z - \bar{p}\right) A_z\Delta_z \cdots\cdots \left(\frac{J}{m^2}\right) \quad (1)$$

A_0 is the lake surface area, $\bar{p}$ is the mean density, $z_{\bar{p}}$ is the depth to the centre of gravity of the water column, A_z is the area at depth z, z_0 is the water surface depth, z_m is the maximum depth, Δ_z is the layer thickness, $A_z \times \Delta_z$ is the volume of the layer (Idso, 1973).

Lake Number (Ln)

The lake number (L_n) can be used to predict lake stability if the water column is mixing due to wind forcing (equation 2). A $L_n = 1$ indicated that the wind is just sufficient to force the thermocline to be deflected to the surface at the upwind end of the lake. For $L_n \geq 1$ and $L_n \leq 1$, the stratification will be expected to be strong and weak, respectively, with respect to the force by wind stress.

$$L_n = \frac{g\, S_t\left(1-\frac{Z_t}{Z_m}\right)}{\rho_0 u^2 A_0 3/2\left(1-\frac{Z_g}{Z_m}\right)} \quad (2)$$

where g is the acceleration of gravity, S_t is the Schmidt stability (from equation 1), Z_t is the thermocline height (m) from the bottom. Z_m is the maximum depth of the water body, ρ_o is the water density at the surface, u^2 is the water friction velocity due to wind speed, A_o and Z_f is the surface area and the height to the centre of volume of the lake in meters off the bottom, respectively (Robertson & Imberger, 1994). The local wind speed data used in this study were obtained from a global model as proposed by Zippenfenig (2024) and the summary data is provided in Supplementary Table S1.

Epilimnion and hypolimnion layer temperatures were determined by measuring the volumetrically weighted average temperature of the top and bottom of the metalimnion in a stratified lake. The thermocline depth was identified as the depth where the temperature decreases by at least 1°C per meter. The metalimnion, characterised by the steepest thermal gradient is delineated between the bottom of the epilimnion and the top of the hypolimnion. All these parameters - thermocline depth and thickness, epilimnion, hypolimnion, and metalimnion temperature, Schmidt stability index (S_t) and lake number (Ln) were computed using the statistical software package R, specifically employing *rLakeAnalyzer*. For detailed instructions on the *rLakeAnalyzer* software, refer to (Winslow *et al*., 2019). The boxplots, correlation plots, PCA-3D, and heat diagram visualisation were built based on *ggplot2*, *ggcorrplot, Excel 3D Scatter Plot*, and *Ocean Data View*, respectively.

Statistical Analysis

Significance (Wilcoxon signed-rank test *p-value*) is based on the distribution of the data over time and is estimated using non-parametric linear regression analysis. If the *p-value* exceeds 0.05 (5%), we conclude that there is no meaningful difference between the paired observations in the dataset.

Results and Discussion

Temporal, Spatial, and Vertical Profiles of Measured Water Parameters

The vertical profiles of temperature, Dissolved Oxygen (DO), dissolved nutrients, and particulate organic carbon are shown in Figure 2. The surface temperature for both littoral and limnetic sites ranged from 31.2°C to 31.7°C [Figure 2 (a and i)]. The temperature remains constant from 30 m down to the bottom, ranging from 23.6°C to 24.2°C. Dissolved oxygen displayed similar trends between littoral and limnetic sites [Figure 2 (b and j)], with the reservoir water saturated with oxygen to a depth of 10 m (> 80% DO), then, start to decrease gradually to reach 10% DO below 20 m.

Dissolved Inorganic Nitrogen (DIN = nitrate + nitrite + ammonium) presented low concentrations in the surface layer (60 ± 36 µg/L). In the littoral zone, DIN concentrations increased with depth, from a mean of 95 ± 46 µg/L at the metalimnion to 243 ± 242 µg/L below 20 m. The vertical profile of DIN in limnetic showed no specific trends, with a few hotspots where the concentration exceeded 500 µg/L in the water column Figure 2 (c). Seasonally, the distribution of DIN concentrations in the Kenyir Reservoir showed no significant differences. Figure 3 (a) also indicates that the median value of DIN concentration in the limnetic zone was significantly higher than in the littoral zone during the dry season ($p < 0.05$, Wilcoxon signed-rank test).

Dissolved Reactive Phosphorus (DRP) concentrations were uniformly low throughout the water column, consistently measuring below 30 µg/L [Figure 2 (d) and (l)]. In the limnetic zone, median DRP concentrations were 5.5 µg/L during dry periods and 8.0 µg/L during wet periods. These concentrations were slightly higher compared to the littoral zone, where median DRP values were 5.3 µg/L during dry periods and 7.3 µg/L during wet periods [Figure 3 (b)]. Spatially, DRP concentration shows no significant difference ($p > 0.05$, Wilcoxon signed-rank test).

The median Dissolved Organic Carbon (DOC) concentrations in both the limnetic and littoral zones ranged from 1.9-2.2 mg/L and 2.1-2.3 mg/L, respectively, across both seasons. For Particulate Organic Carbon (POC), the median concentrations in the littoral and limnetic zones ranged from 1.3-2.7 mg/L and 1.2-2.9 mg/L, respectively. Both DOC and POC showed no significant variation with depth in the water columns [Figure 2 (e), (f), (m), and (n)] but exhibited significant concentration differences between the dry and wet seasons [Figure 2 (d) and (e), $p < 0.05$, Wilcoxon signed-rank test]. Higher POC concentrations during the wet season are attributed to runoff, with increased POC likely driven by terrestrial debris from the surrounding forested landscape, which is the major land use. In contrast, lower DOC concentrations during the wet season result from dilution by rainfall and surface water flow.

Figure 2 (h) and Figure 2 (p) demonstrate that the vertical and spatial variation of CH_4 concentrations in the reservoir varied by more than one order of magnitude, ranging from 0.1 µM to 1,346 µM. Notably, there is a significant difference in CH_4 concentrations between the surface and the bottom, with measurements below 20 m depth exceeding 250 µM. The average CH_4 concentration in the limnetic zone was 186 ± 247 µM while in the littoral zone, the average CH_4 concentration was 39 ± 188 µM. The CH_4 concentration at the bottom was significantly higher than that observed at the surface.

Carbon dioxide (CO_2) exhibited a trend similar to that of CH_4, with the greatest differences between surface and bottom concentrations observed in all sampled seasons [Figure 2 (g) and (o)]. Figure 3 (f) illustrates that in the limnetic zone, CO_2 concentration shows no significant seasonal differences. However, in the littoral zone, CO_2 concentration shows a substantial difference between the dry (median = 207 µM) and wet periods (median = 161 µM).

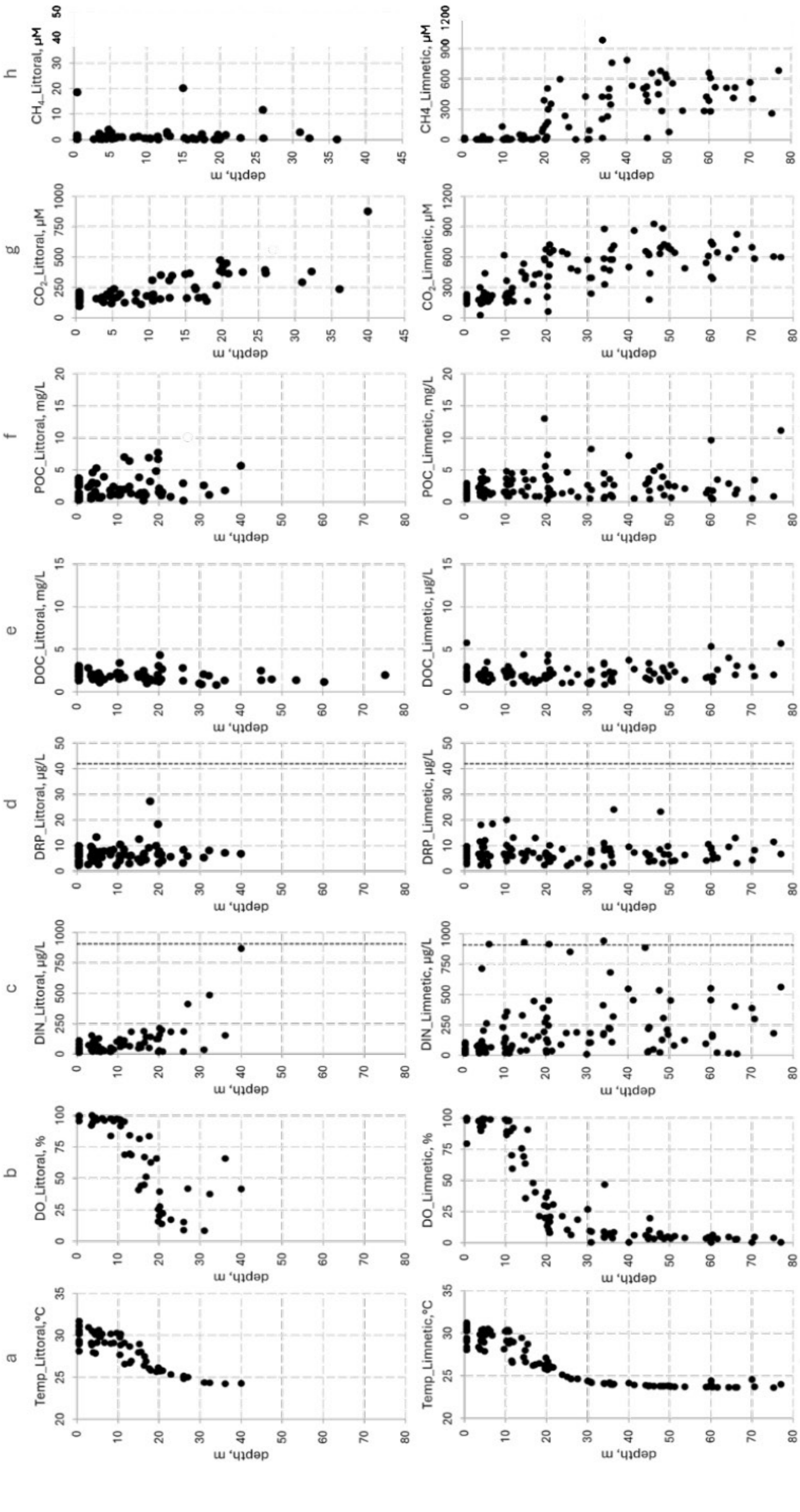

Figure 2: Depth profiles of temperature, dissolved oxygen, nutrients, and greenhouse gases at littoral (top panel) and limnetic sites (below panel). The red dashed line indicates the global average value

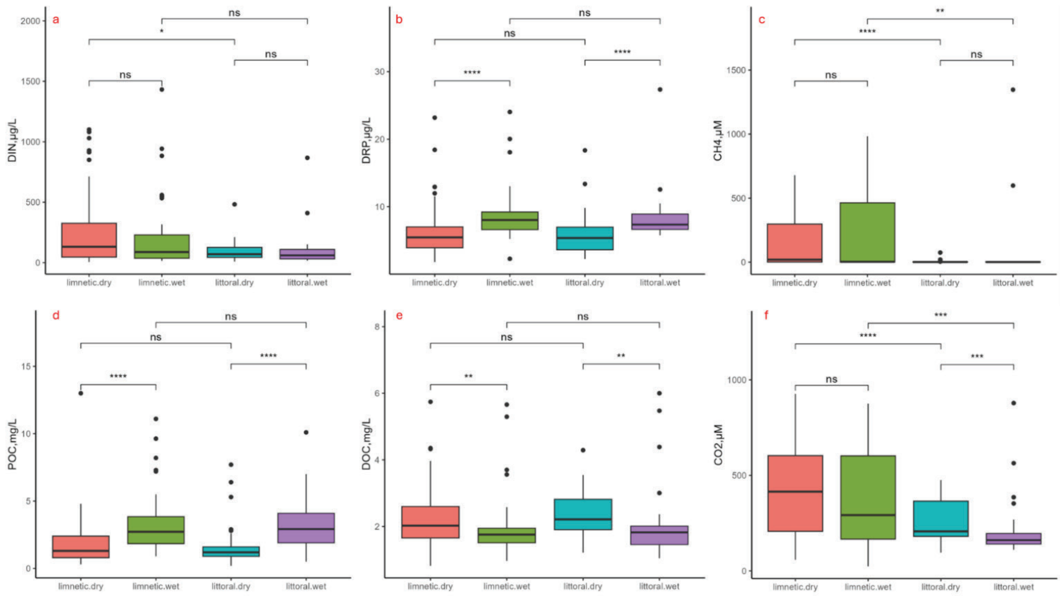

Figure 3: Boxplots representing differences in DIN, DRP, POC, DOC, CH_4, and CO_2 concentration between limnetic and littoral sites during dry and wet seasons in Kenyir Reservoir

Thermal Stratification of Kenyir Reservoir

The Kenyir reservoir was thermally stratified throughout the study period (Table 2 & Figure 4). During the dry period from March to July 2018, average thermocline depths at both littoral and limnetic sites were observed at 26.9 ± 2.3 m and 24.4 ± 1.9 m, respectively (Table 2). During the wet periods (February and November 2018), the thermocline depths were similar, ranging from 26.1 ± 1.9 m at the littoral zone to 25.4 ± 2.4 m at the limnetic zone. Figure 4 (a) and Figure 4 (c) show that the vertical water column temperature in both littoral and limnetic sites varies from 2°C to 5°C. Table 2 shows that the average epilimnion temperature during the dry period was slightly higher compared to the wet period.

Meanwhile, the thermocline layer temperature remained consistent at 25 ± 1°C throughout the reservoir. At the bottom layer, temperatures in both limnetic and littoral zones remained consistent seasonally, but the hypolimnion temperature in the limnetic zone was found to be at least 1°C lower than in the littoral zone. Table 2 shows no difference in thermocline thickness between limnetic and littoral sites. However, the average metalimnion thickness in the littoral zone decreased by half during the wet season, likely due to cooler atmospheric temperatures, increased wind, and runoff, which enhance surface mixing. Figure 4 (a-c) shows that short periods of cool, windy weather (February and November 2018, see supplementary Table S1) can temporarily deepen the mixed layer without disrupting deeper stratification. Vertical mixing in stratified waters is driven by turbulent diffusivity, controlled by wind energy and water column stability (Vachon *et al*., 2019). Like other deep-water bodies, Kenyir Reservoir exhibits a stable thermal structure with a well-mixed upper layer separated from a colder bottom layer (Yusoff & Lock, 1995).

The Schmidt Stability Index (St) and lake number (Ln) are widely used to describe lake stratification intensity. St measures the energy required to mix the entire water column to uniform temperatures without changing its internal energy (Ladwig *et al*., 2021). Ln reflects the balance between stabilising forces such as gravity from density stratification and destabilising forces, including wind, cooling, inflow, outflow, and artificial mixing (Robertson & Imberger, 1994).

Table 2 highlights the stratification dynamics of the Kenyir reservoir, with St values ranging from 1,422 J/m^2 to 8,450 J/m^2, depending on depth and season. During the wet season, Ln values decrease across the lake, from 6 to 41, compared to higher dry-season values of 35 to 43. This reduction indicates weakened stratification during the wet monsoon, driven by stronger wind forces and increased mixing. However, the high energy required for full mixing suggests that a complete lake overturn is unlikely.

Like other tropical deep-water lakes (Winton *et al.*, 2019), Kenyir Reservoir remains thermally stratified year-round due to its stable water level (≥ 120 m) and minimal inflow and outflow, except during heavy rainfall (Mohd Sidek *et al.*, 2020). The persistent stratification observed in Kenyir is consistent with findings from Yusoff (2008) and Rouf *et al.* (2008), who reported similar trends in tropical reservoirs.

Table 2: Comparison of *rLakeAnalyzer* calculations for thermocline depth, metalimnion thickness, lake number, Schmidt stability, and reservoir water temperature measurements during dry and wet seasons

	Dry		**Wet**	
	Littoral (n = 8)	**Limnetic (n = 12)**	**Littoral (n = 4)**	**Limnetic (n = 7)**
Thermocline depth (m)	26.9 ± 2.3	24.4 ± 1.9	26.1 ± 1.9	25.4 ± 2.4
Thermocline thickness (m)	4.4 ± 1.2	5.3 ± 1.2	2.5 ± 1.1	4.3±0.9
Schmidt stability (J/m^2)	5114 ± 1435	7280 ± 1170	3011 ± 1589	5912 ± 1342
Lake Number	26 ± 9	34 ± 9	10 ± 4	28 ± 13
Epilimnion temperature (°C)	30.2 ± 0.7	29.6 ± 0.5	28 ± 0.7	28.2 ± 0.6
Metalimnion temperature (°C)	25.6 ± 1	25.1 ± 0.4	25.8 ± 1.1	25.3 ± 0.3
Hypolimnion temperature (°C)	26.4 ± 0.8	24.8 ± 0.5	26.1 ± 1.2	24.9 ± 0.5

n represents the number of depth profiles.

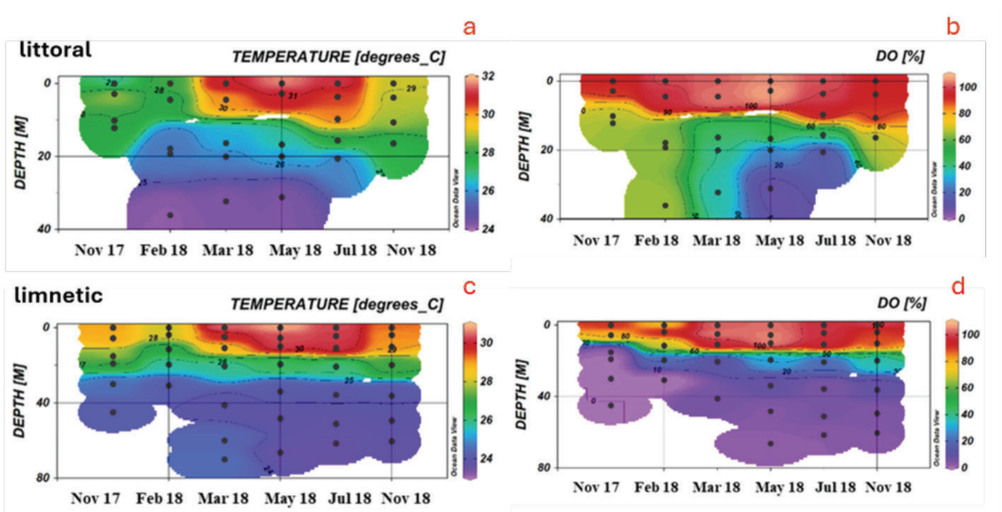

Figure 4: Temporal and depth profiling of temperature and dissolved oxygen between S1 (littoral) and S4 (limnetic) in Kenyir Reservoir

High solar radiation in the tropics contributes to greater surface water temperatures, reinforcing stratification, and reducing vertical mixing. Additionally, Yusoff (2008) noted that monsoonal rainfall and inflow dynamics can influence stratification strength. While Kenyir follows these general patterns, localised hydrodynamic factors such as inflow patterns and wind-driven mixing may further modulate its thermal structure.

Effects of Thermal Stratification on Water Quality Parameters

We used Principal Component Analysis (PCA) to relate the physical and chemical variables to water column depths. Before performing PCA, the Kaiser-Meyer-Olkin (KMO) measure of sampling adequacy was 0.79 and Bartlett's test of sphericity was significant ($p < 0.01$), indicating that the data was appropriate for PCA. The PCA explains 70.9% of the total variation in the dataset, as shown in Table 3. The coloured spheres in Figure 5 represent distinct sampling months, indicating temporal variability in water characteristics. In general, the 3D PCA plot identified three different clusters of samples (spheres) represented by red, blue, and black ovals. If spheres within clusters of similar colours are observed, it suggests consistent conditions within certain months.

Principal Component 1 (PC1) accounting for 43% of the total variance, shows significant positive loadings for depth, CH_4 (0.83), and CO_2 (0.91), negative loadings for temperature (-0.95) and dissolved oxygen (-0.93) (Table 2). The red oval highlights this relationship. The findings indicate that elevated CO_2 and CH_4 concentrations are associated with greater greenhouse gas production at anoxic hypolimnion.

Principal Component 2, accounting for 14.6% of the total variance is dominated by Dissolved Organic Carbon (DOC) (0.832) and Particulate Organic Carbon (POC) (0.827) indicates organic carbon content plays a key role in sample separation along this axis as the human activity such as agriculture, deforestation, and tourism are causing the debris can enter the lake during raining (Kamarudin *et al*., 2018). The high PC2 loading observed for the sample represents blue spheres in February 2018, suggesting significant organic input from the nearby area. Heavy rains earlier in the wet season may have eroded forest floors and

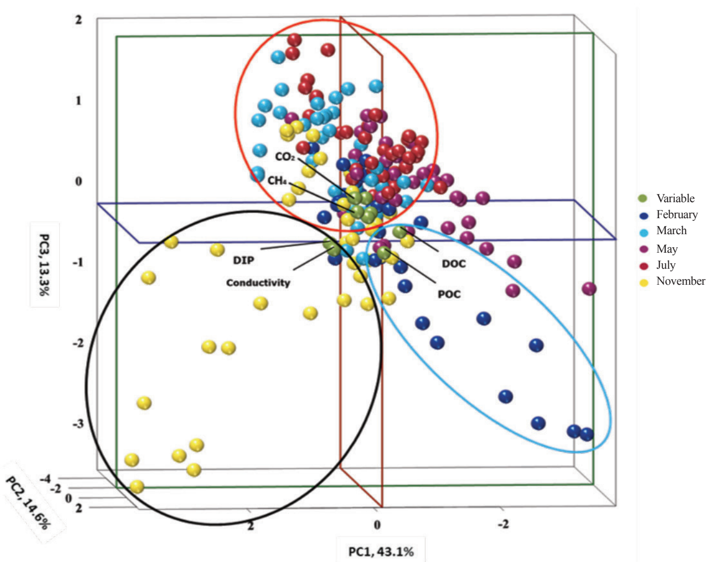

Figure 5: 3D PCA scatter plots of the first three principal components derived from datasets analysing the water quality characteristics of each sample. The groups are colour-coded according to the sampling month. The green dots are the loadings

Table 3: Principal Component Analysis (PCA) of the water quality and greenhouse gas species

	PC Component		
Input	**PC1**	**PC2**	**PC3**
O_2 saturation	-0.934		
Sample depth	0.926		
Temperature	-0.925		
CO_2 saturation	0.912		
CH_4 saturation	0.826	0.217	
Dissolved Inorganic Nitrogen (DIN)	0.427	0.105	-0.148
Dissolved Organic Carbon (DOC)		0.832	-0.263
Dissolved Reactive Phosphorus (DRP)			0.779
Particulate Organic Carbon (POC)	0.156	0.827	0.157
Conductivity			0.770
Eigenvalues	4.31	1.46	1.33
Variance per component (%)	43.1	14.6	13.3
Cumulative variance (%)	43.1	57.7	70.9

brought organic debris downstream with much of it accumulating near the reservoir by the end of the wet season. Substantial organic debris from the terrestrial environment being flushed into the reservoir inflowing areas via rainfall events during the wet season is a commonly reported phenomenon (Zhang *et al*., 2024).

Principal Component 3 (PC3) shows high loadings of DRP and electrical conductivity for some of the yellow spheres in the black oval, representing samples collected from the epilimnion during the November 2018 sampling. The November 2018 sampling coincided with the onset of the monsoon season, characterised by stronger winds compared to other sampling months (Table S1). These winds likely caused initial mixing only in the upper layers, causing DRP and ion redistribution in the epilimnion while leaving the hypolimnion undisturbed. The reduction in metalimnion thickness during November 2018 [Figure 4 (a) and (c)] further supports this, as at the start of the wet season, mixing may not be strong enough to homogenise the water column fully.

Our result shows that the vertical variation of dissolved oxygen concentration was closely coupled to the thermal stratification of Kenyir Reservoir. Figure 4 (b and d) shows that the reservoir was almost 100% oxygen saturation at the surface. The oxygen saturation decreases with depth, reaching about 50% at 20 m in the hypolimnion layer. In the limnetic zone, at depths greater than 40 m, the measured oxygen saturation level drops to less than 10%. Dissolved oxygen in lakes plays an important role in nutrient biogeochemical cycles.

Furthermore, dissolved oxygen can affect and regulate the biogeochemical cycles of freshwater ecosystems through shifting the redox potential. Studies showed that the concentration of dissolved oxygen affects the activity of the microbial communities (Yang *et al*., 2021), inorganic nutrients assimilation within the water column (Yue *et al*., 2023) and organic matter mineralisation in lake sediment (Steinsberger *et al*., 2020). In the case of nutrient availability in lake sediment, nutrient consumption rates are generally much greater under anoxic conditions (Osaka *et al*., 2022).

In Kenyir Reservoir, most measured nutrients, except the Dissolved Inorganic Nitrogen (DIN) were uniformly distributed throughout the water column [Figure 2 (c) and (k)]. Dissolved nitrogen concentration in the limnetic zone ranged from 5 µg/L to over 500 µg/L, with a few high anomalies observed in the thermocline depth [Figure 2 (k)]. These high anomaly concentrations were above the world freshwater average of 908 µg/L reported by Filazzola *et al*. (2020). We postulated that the higher upstream input/ runoff during the wet period caused the elevated dissolved nitrogen concentration in the upper layer of water in the stratified lake (epilimnion). The DIN vertical profile in littoral, on the other hand, shows an increasing trend with depth. Suratman *et al.* (2017) reported similarly dissolved nitrogen levels in Kenyir Reservoir (nitrate: 12.5 µg/L – 111.6 µg/L, ammonia: 6.1 µg/L – 88.4 µg/L), classifying the reservoir as Class I under Malaysia's National Water Quality Standard. Low DRP [Figure 2 (d) and (l)] confirms the reservoir's oligotrophic status, consistent with Suratman *et al.* (2015).

The average concentrations of dissolved phosphorus and nitrogen throughout the sampling campaign were at least one order of magnitude lower than the global freshwater lake average (Filazzola *et al*., 2020). The stability of nutrient levels over time suggests that Kenyir Reservoir experiences minimal anthropogenic input or significant internal nutrient cycling. This reinforces its classification as a relatively pristine water body with low eutrophication risk. However, localised anomalies in DIN at the thermocline indicate potential seasonal influences such as upstream runoff during wet periods, which could affect nutrient availability and primary productivity.

Due to the presence of outliers in the CH_4 and CO_2 dataset median value was used for seasonal and temporal comparison, the median CH_4 and CO_2 concentrations in Kenyir were usually higher in the dry period (CH_4 = 1.8 µM, CO_2 = 309 µM), compared with the wet period (CH_4 = 1.2 µM, CO_2 = 175 µM). Spearman's correlation between GHGs showed evidence of a stronger linear effect of CH_4 on the CO_2 during the dry period (r = 0.8, $p < 0.05$), compared to the wet period (r = 0.5, $p < 0.05$), see supplementary Figure 2. Figure 6 shows that the CO_2 to CH_4 concentration ratio begins to increase exponentially at depths shallower than 20 meters. In oxygenated water columns, the aerobic methanotrophic bacteria use molecular oxygen to oxidise methane to CO_2 (Oswald *et al*., 2016). Our result suggests that the methane oxidation process may induce greater CO_2 production in the mixing layer.

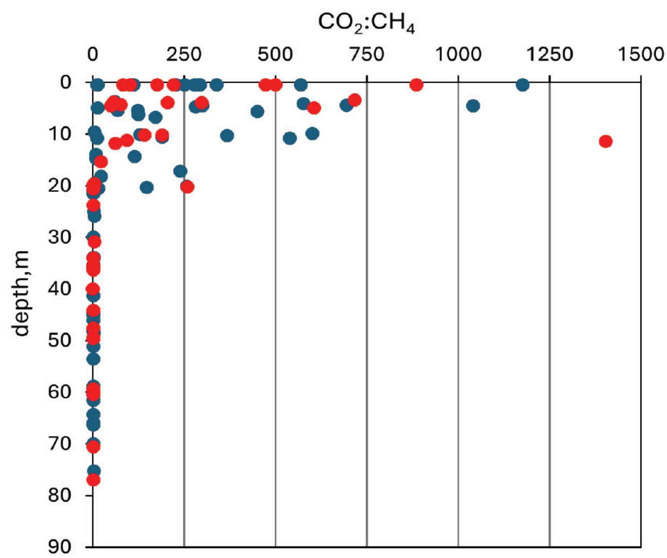

Figure 6: Depth profile of CO_2:CH_4 ratio at Kenyir Reservoir. Blue and red dots represent wet and dry seasons, respectively

Under current conditions, turnover in Kenyir Reservoir is unlikely, leading to sustained greenhouse gas storage in deeper waters. However, climate change may alter this stability. Shifts in precipitation patterns could weaken thermal stratification, potentially enhancing oxygen penetration but also disrupting carbon storage dynamics. Conversely, prolonged droughts or extreme rainfall events may cause abrupt water level fluctuations, increasing the likelihood of episodic mixing and greenhouse gas release (Tranvik *et al*., 2016).

From a management perspective, this finding emphasises the need for continuous water quality monitoring, particularly by tracking the migration of the anoxic layer, which influences GHG production and organic matter oxidation dynamics. Additionally, controlling reservoir water levels could help regulate stratification patterns and limit prolonged anoxic conditions, thereby reducing CH_4 accumulation in deeper layers.

Conclusions

The stability of water stratification in Kenyir Reservoir has both physical and chemical implications. Dissolved nutrients in Kenyir Reservoir were generally well-distributed throughout the water column during the study period, though some variation was observed in the vertical profile of dissolved inorganic nitrogen. Both the lake number and Schmidt stability index suggest that thermal stratification in Kenyir reservoir is likely to persist, as the reservoir experiences strong thermal stratification throughout the year. Dissolved oxygen saturation level decreases to less than 10% at depths beyond 40 m, leading to anoxic conditions in deeper waters. Our result indicates that turnover in the Kenyir Reservoir is very unlikely. This could potentially result in much higher greenhouse gas production, with these gases reaching the surface through diffusion or ebullition.

Given Kenyir Reservoir's role in hydropower and regional water resources, Tenaga Nasional Berhad (TNB) and the Central Terengganu Development Authority (KETENGAH)–the primary agencies overseeing Kenyir reservoir long-term water management should prioritise water quality monitoring, controlled reservoir levels to limit anoxic layer expansion, and optimised dam operations to prevent sudden destratification.

As climate variability influences rainfall patterns and water levels, future projections under the IPCC's worst-case scenario (RCP8. 5) suggest that rainfall intensity and extremes over Peninsular Malaysia are likely to decrease during the Northeast monsoon and increase during the Southwest monsoon by the end of the century (Ngai *et al.*, 2020). These changes could exacerbate hydrological variability, intensify reservoir stratification, and influence carbon emissions. Integrating these findings into adaptive management strategies will help mitigate potential impacts on water quality, ecosystem health, and hydropower sustainability.

Acknowledgements

This work was funded by the Malaysia Ministry of Higher Education-Fundamental Research Grant Scheme (FRGS/1/2015/WAB05/UMT/02/1).

Conflict of Interest Statement

The authors declare that they have no conflict of interest.

References

Abdul Razad, A., Samsudin, S. H., Abbas, N., Setu, A., Mohd Sidek, L., Jung, K., & Sharip, Z. (2020). Sediment yield modeling as sediment management strategies towards sustainability of hydropower reservoirs in Malaysia. *ICDSME*, *2019*, 26-37. DOI: 10.1007/978-981-15-1971-0_4

Ambak, M. A., & Jalal, K. C. A. (1998). Habitat utilisation by the tropical fish community in the man-made Lake Kenyir, Malaysia. *Fisheries Management and Ecology*, *5*, 173-176. DOI: 10.1046/j.1365-2400.1998.00 097.x

Barillé-Boyer, A. L., Barillé, L., Massé, H., Razet, D., & Héral, M. (2003). Correction for particulate organic matter as estimated by loss on ignition in estuarine ecosystems. *Estuarine, Coastal and Shelf Science*, *58*(1), 147-153. DOI: 10.1016/s0272-7714(03)00 069-6

Beaulieu, J. J., Smolenski, R. L., Nietch, C. T., Townsend-Small, A., Elovitz, M. S., & Schubauer-Berigan, J. P. (2014). Denitrification alternates between a source and sink of nitrous oxide in the hypolimnion of a thermally stratified reservoir. *Limnology and Oceanography*, *59*, 495-506. DOI: 10.4319/LO.2014.59.2.0495

DelSontro, T., Boutet, L., St-Pierre, A., del Giorgio, P. A., & Prairie, Y. T. (2016). Methane ebullition and diffusion from northern ponds and lakes regulated by the interaction between temperature and system productivity. *Limnology and Oceanography*, *61*, S62-S77. DOI: 10.1002/lno.10335

Filazzola, A., Mahdiyan, O., Shuvo, A., Ewins, C., Moslenko, L., Sadid, T., Blagrave, K., Imrit, M. A., Gray, D. K., Quinlan, R., O'Reilly, C. M., & Sharma, S. (2020). A database of chlorophyll and water chemistry in freshwater lakes. *Scientific Data*, *7*, 310. DOI: 10.1038/s41597-020-00648-2

García-Robledo, E., Corzo, A., & Papaspyrou, S. (2014). A fast and direct spectrophotometric method for the sequential determination of nitrate and nitrite at low concentrations in small volumes. *Marine Chemistry, 162*, 30-36. DOI: 10.1016/j.marchem.2014.03.002

Idso, S. B. (1973). On the concept of lake stability. *Limnology and Oceanography*, *18*, 681-683. DOI: 10.4319/lo.1973.18.4.0681

Kamaruddin, I. S., Kamal, A. S. M., Christianus, A., Daud, S. K., & Abit, L. Y. (2011). Fish community in Pengkalan Gawi – Pulau Dula Section of Kenyir Lake, Terengganu, Malaysia. *Journal of Sustainability Science and Management, 6*(1), 89-97.

Ladwig, R., Hanson, P. C., Dugan, H. A., Carey, C. C., Zhang, Y., Shu, L., Duffy, C. J., & Cobourn, K. M. (2021). Lake thermal structure drives interannual variability in summer anoxia dynamics in a eutrophic lake over 37 years. *Hydrology and Earth System Sciences, 25*, 1009-1032. DOI: 10.5194/hess-25-1009-2021

Lee, D. J. J., Kek, K. T., Wong, W. W., Mohd Nadzir, M. S., Yan, J., Zhan, L., & Poh, S. C. (2022). Design and optimisation of wireless in-situ sensor coupled with gas–water equilibrators for continuous pCO_2 measurement in aquatic environments. *Limnology Oceanography: Methods*, *20*, 500513. doi.org/10.1002/lom3.10500

Ma, S-N., Wang, H-J., Wang, H-Z., Zhang, M., Li, Y., Bian, S-J., Liang, X-M., Søndergaard, M., & Jeppesen, E. (2021). Effects of nitrate on phosphorus release from lake sediments. *Water Research*, *194*, 116894. DOI: 10.1016/j.watres.2021.116894

Mohd Sidek, L., Razali, J., Marufuzzaman, M., Yalit, M. R., Radzi, M. R. M., & Shabbir Hossain, M. (2020). Flood hydrograph generation for Kenyir Dam using hydrological modeling system. In Mohd Sidek, L., Salih, G. H. A., & Boosroh, M. H. (Eds.), *ICDSME 2019* (pp. 64-75). Singapore: Springer.

Noori, R., Berndtsson, R., Franklin Adamowski, J., & Rabiee Abyaneh, M. (2018). Temporal and depth variation of water quality due to thermal stratification in Karkheh Reservoir, Iran. *Journal of Hydrology: Regional Studies*, *19*, 279-286. https://doi.org/10.1016/j.ejrh.2018.10.003

Ngai, S. T., Juneng, L., Tangang, F., Chung, J. X., Salimun, E., Tan, M. L., & Amalia, S. (2020). Future projections of Malaysia daily precipitation characteristics using bias correction technique. *Atmospheric Research*, *240*(104926). DOI: 10.1016/j.atmosres.2020.104926

Osaka, K., Yokoyama, R., Ishibashi, T., & Goto, N. (2022). Effect of dissolved oxygen on nitrogen and phosphorus fluxes from lake sediments and their thresholds based on incubation using a simple and stable dissolved oxygen control method. *Limnology and Oceanography: Methods*, *20*, 1-14. DOI: 10.1002/lom3.10466

Oswald, K., Jegge, C., Tischer, J., Berg, J., Brand, A., Miracle, M. R., Soria, X., Vicente, E., Lehmann, M. F., Zopfi, J., & Schubert, C. J. (2016). Methanotrophy under versatile conditions in the water column of the Ferruginous Meromictic Lake La Cruz (Spain). *Frontiers in Microbiology*, *7*(NOV), 1-16. DOI: 10.3389/fmicb.2016.01762

Pu, J., Li, J., Zhang, T., Martin, J. B., & Yuan, D. (2020). Varying thermal structure controls the dynamics of CO_2 emissions from a subtropical reservoir, south China. *Water Research*, *178*, 115831. DOI: 10.1016/j.watres.2020.115831

Robertson, D. M., & Imberger, J. (1994). Lake number, a quantitative indicator of mixing used to estimate changes in dissolved oxygen. *Internationale Revue der gesamten Hydrobiologie und Hydrographie*, *79*, 159-176. DOI: 10.1002/iroh.19940790202

Rouf, A. J. M. A., Ambak, M. A., Shamsudin, L., Phang, S-M., & Ho, S. C. (2008). Temporal changes in the periphytic algal communities in a drowned tropical forest reservoir in Malaysia: Lake Kenyir. *Lakes & Reservoirs: Science, Policy and Management for Sustainable Use*, *13*, 271-287. DOI: 10.1111/j.1440-1770.2008.00382.x

Rouf, A. J. M. A., Phang, S-M., & Ambak, M. A. (2010). Depth distribution and ecological preferences of periphytic algae in Kenyir Lake, the largest tropical reservoir of Malaysia. *Chinese Journal of Oceanology and Limnology*, *28*, 856-867. DOI: 10.1007/s00343-010-9088-0

Sharip, Z. (2017). Stratification and water quality variations in three large tropical reservoirs. *International Journal of Ecology and Environmental Sciences*, *43*, 175-184.

Steinsberger, T., Schwefel, R., Wüest, A., & Müller, B. (2020). Hypolimnetic oxygen depletion rates in deep lakes: Effects of trophic state and organic matter accumulation. *Limnology and Oceanography*, *65*, 3128-3138. DOI: 10.1002/lno.11578

Sultan, K., & Shazili, N. A. (2009a). Rare earth elements in tropical surface water, soil and sediments of the Terengganu River Basin, Malaysia. *Journal of Rare Earths*, *27*, 1072-1078. DOI: 10.1016/S1002-0721(08)60391-9.

Sultan, K., & Shazili, N. A. (2009b). Distribution and geochemical baselines of major, minor and trace elements in tropical topsoils of the Terengganu River basin, Malaysia. *Journal of Geochemical Exploration*, *103*, 57-68. DOI: 10.1016/j.gexplo.2009.07.001

Suratman, S., Bedurus, E., & Hock Seng, T. (2017). A preliminary study of the distribution of nitrogen compounds in tasik kenyir, Malaysia. *Oriental Journal of Chemistry*, *33*(3), 1325-1330. DOI: 10.13005/ojc/330332

Suratman, S., Hee, Y. Y., & Hock Seng, T. (2015). A preliminary study of the distribution of phosphorus and silicon compounds in Tasik Kenyir, Hulu Terengganu, Malaysia. *Journal of Sustainability Science and Management*, *10*(2), 35-41.

Tranvik, L. J., Downing, J. A., Cotner, J. B., Loiselle, S. A., Striegl, R. G., Ballatore, T. J., … Weyhenmeyer, G. A. (2009). Lakes and reservoirs as regulators of carbon cycling and climate. *Limnology and Oceanography*, *54*. https://doi.org/10.4319/lo.2009.54.6_part_2.2298

USEPA. (1993). *Method 350.1: Nitrogen, Ammonia by Colorimetric, Automated Phenate*, Revision 2.0. Cincinnati, OH.

USEPA. (1993). *Method 365.1: Determination of Phosphorus by Semi-Automated Colorimetry*, Revision 2.0. Cincinnati, OH.

USEPA. (2002). *Methods for Evaluating Wetland Condition: Wetlands Classification*. Office of Water, U.S. Environmental Protection Agency, Washington, DC. EPA-822-R-02-01

Vachon, D., Langenegger, T., Donis, D., & McGinnis, D. F. (2019). Influence of water column stratification and mixing patterns on the fate of methane produced in deep sediments of a small eutrophic lake. *Limnology and Oceanography*, *64*, 2114-2128. DOI: 10.1002/lno.11172

Wahab, N. A., Kamarudin, M., Toriman, M., Juahir, H., Ata, F., Ghazali, A., Samah, M., Azinuddin, M., Khairuldin, W., & Hoe, L. (2022). The assessment of sedimentation and water quality status for river catchment management in Kenyir Lake Basin. *Desalination and Water Treatment, 269*, 93-105. DOI: 10.5004/dwt.2022.28674

Wahab, N. A., Kamarudin, M. K. A., Toriman, M. E., Juahir, H., Samah, M. A. A., Azinuddin, M., Saudi, A. S. M., Hoe, L. I., Saad, M. H. M., & Sunardi, S. (2023). The assessment of sedimentation problems in Kenyir Hydropower Reservoir, Malaysia. *Water*, *15*, 2375. DOI: 10.3390/w15132375

Wang, H., Li, Y., Li, Y., Liu, H., Wang, W., Zhang, P., Fohrer, N., Li, B-L., & Zhang, Y. (2024). Phytoplankton communities' response to thermal stratification and changing environmental conditions in a deep-water reservoir: Stochastic and deterministic processes. *Sustainability*, *16*. DOI: 10.3390/su16073058

Winslow, L., Read, J., Woolway, R., Brentrup, J., Leach, T., Zwart, J., Albers, S., & Collinge, D. (2019). *rLakeAnalyzer: Lake Physics Tools*. R package version 1.11.4.1.

Winton, R. S., Calamita, E., & Wehrli, B. (2019). Reviews and syntheses: Dams, water quality and tropical reservoir stratification. *Biogeosciences*, *16*, 1657-1671. DOI: 10.5194/bg-16-1657-2019

Yang, N., Zhang, C., Wang, L., Li, Y., Zhang, W., Niu, L., Zhang, H., & Wang, L. (2021). Nitrogen cycling processes and the role of multi-trophic microbiota in dam-induced river-reservoir systems. *Water Research*, *206*, 117730. DOI: 10.1016/j.watres.2021.117730

Yue, Y., Yang, Z., Cai, L., Bai, C., Huang, Y., Ma, J., & Yang, M. (2023). Effects of stratification and mixing on spatiotemporal dynamics and functional potential of microbial community in a subtropical large-deep reservoir driven by nutrients and ecological niche. *Ecological Indicators*, *156*, 111128. DOI: 0.1016/j.ecolind.2023.111128

Yusoff, F. M. (2008). Tasik Kenyir: Thermal stratification and its implications on sustainable management of the reservoir. In Anton, A. (Ed.), *Lakes and reservoir management* (pp. 89-99). NAHRIM, Seri Kembangan.

Yusoff, F. M., & Lock, M. A. (1995). Thermal stratification and its role in controlling eutrophication in a tropical reservoir, Malaysia. In Timotius, K. H., & Goltenboth, F. (Eds.), *Tropical Limnology. Vol. II. Tropical lakes and reservoirs* (pp. 277-285). Salatiga, Indonesia.

Yusoff, F. M., Matias, H. M., & Khan, N. (2002). Changes of water quality, chlorophyll a and zooplankton along the river-lacustrine continuum in a tropical reservoir. *SIL Proceedings 1922-2010*, *28*, 295-298. DOI: 10.1080/03680770.2001.11902590

Zhang, T., Zhou, L., Zhou, Y., Zhang, Y., Guo, J., Han, Y., Zhang, Y., Hu, L., Jang, K., Spencer, R. G., Brookes, J. D., Dolfing, J., & Jeppesen, E. (2024). Terrestrial dissolved organic matter inputs accompanied by dissolved oxygen depletion and declining pH exacerbate CO_2 emissions from a major Chinese reservoir. *Water Research*, *251*, 121155. DOI: 10.1016/j.watres.2024.121155

Zhou, Y., Zhou L, Zhang, Y., Garcia de Souza, J., Podgorski, D. C., Spencer, R. G., Jeppesen, E., & Davidson, T. A. (2019). Autochthonous dissolved organic matter potentially fuels methane ebullition from experimental lakes. *Water Research*, *166*, 115048. DOI: 10.1016/j.watres.2019.115048

Zippenfenig, P. (2024). *Open-Meteo.com Weather API (1.4.0)*. Zenodo. DOI: 10.5281/zenodo.14582479

Appendices

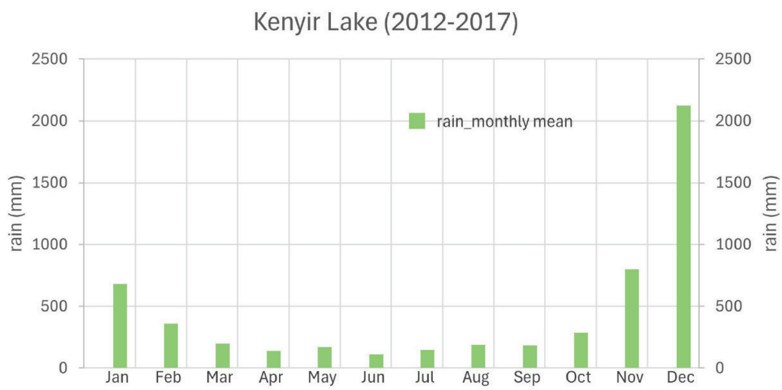

Figure S1: 5-years monthly average rainfall data for Kenyir Reservoir

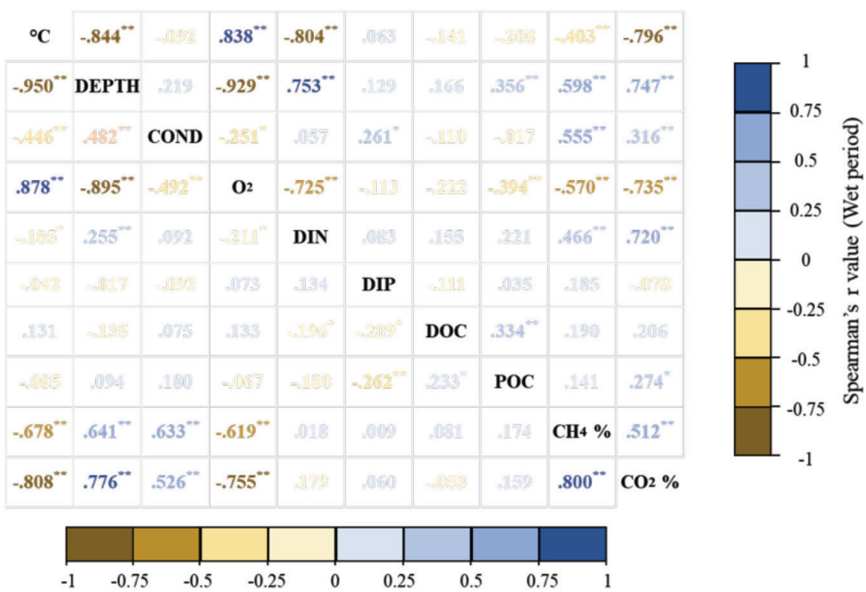

Figure S2: Spearman correlation plot of water quality and GHGs for Kenyir Reservoir

Table S1: Summary of wind speed data for Kenyir Reservoir
(lat:5.015786°, long: 102.848353°)

Month	Average of Wind Speed 10 m (m/s)	Min of Wind Speed 10 m (m/s)	Max of Wind Speed 10 m (m/s)
Jan-18	1.39	0.00	5.24
Feb-18	1.78	0.00	4.92
Mar-18	1.55	0.00	3.94
Apr-18	1.44	0.14	3.94
May-18	1.13	0.00	3.92
Jun-18	1.04	0.00	3.55
Jul-18	0.96	0.00	2.62
Aug-18	1.06	0.00	3.31
Sep-18	1.07	0.00	3.33
Oct-18	1.21	0.10	4.10
Nov-18	1.27	0.00	4.10
Dec-18	1.40	0.10	4.32

Source: Historical local wind data from global models as described in Zippendenig (2023)